

Robust Analysis and Design of Bored Pile Considering Uncertain Parameters

Alimzhan Oteuil¹, Adilbek Oralbek¹, Tileuzhan Mukhamet¹, Sung-Woo Moon¹, Jong Kim¹,
Serik Tokbolat², Alfrendo Satyanaga^{1*}

¹Department of Civil and Environmental Engineering, Nazarbayev University, Nur-Sultan 010000, Kazakhstan

²Department of Construction Management, Nottingham Trent University, 50 Shakespeare street, Nottingham NG1 4FQ, United Kingdom

*Corresponding author: alfrendo.satyanaga@nu.edu.kz

Abstract: Many high-rise buildings and bridges in the worlds are constructed using bored pile. To provide a safe design of this type of deep foundation, high quality soil data is needed which is normally obtained from laboratory testing. However, the contractor and the consultant often conduct only a limited field testing without performing laboratory tests. As a result, the capacity of bored pile may deviate from the real value. This study aims to develop a framework for analysis and design of axial and lateral capacity of bored piles when only a few soil parameters are known. The proposed methodology uses analytical methods backed by numerical calculations according to relevant code of practice. The results indicate that as long as the analytical results are supported by the numerical calculations, a robust design can be achieved with only a few soil parameters: a standard penetration test and a cone penetration test.

Key words: Bored pile, axial capacity, lateral capacity, soil properties

1. Introduction

Geotechnical engineering is a complex field of construction industry with a massive influence on people's lives. Understanding the principles of geotechnical engineering would ease the construction and design of buildings and reduce possible risks. Various geotechnical issues are encountered in the world: earthquakes, landslides, liquefaction, and soil instability [1-4]. One of major geotechnical failures occurred at the Tokyo Bay Area. Liquefaction and improper design of pile foundation were the main cause of construction failure in this area [5].

The usual role of a deep foundation is to transfer vertical loads through weak soils near the surface to strong soils and rock underneath. Bored pile is one of common types of deep foundation, typically used to accommodate excessive loading from tall buildings [6-7]. Study by Brown et al. [8] indicated that the ranges of diameter and depth of bored piles are 1 m to 2.5

33 m and 60-90 m, respectively. Bored piles can be constructed using different methods, such as
34 drilling using shafts, drilling under dry condition, installation of caissons and drilled piers [9-
35 10]. Axial resistance of bored piles is summation of the based and skin resistances of the piles.
36 The most significant limitation of bored piles is sensitivity of its performance to construction
37 procedure and ground conditions [11-12]. The primary objectives of engineering design are
38 safety, serviceability, and economy. Safety and serviceability can be improved by increasing
39 the safety margins and reducing the probability of failure [13-15]. To develop a framework that
40 considers the model uncertainty, a relationship between the parameter, the observation, and the
41 model itself should be clarified [16-18].

42 Previous studies showed that the Standard Penetration Test (SPT) and the Cone
43 Penetration Test (CPT) were commonly used to determine the required soil properties based on
44 empirical correlation to be used in the geotechnical design [19-21]. Total resistances of pile
45 foundation and bearing capacity of shallow foundation have been correlated directly to these
46 in-situ tests without using $\tan \phi'$ and c' parameters. To overcome the limitation related to the
47 empirical correlations used in the determination of geotechnical parameters, the European code
48 introduced a partial factor [22-24].

49 Various theories and models were proposed for geotechnical analysis and design when
50 only a few soil properties are known due to limited soil sampling and site investigation. Past
51 studies have been performed to incorporate the uncertainty of soil properties in the slope design.
52 Alkasawneh et al. [25] concluded that limit equilibrium methods, when coupled with the
53 Monte-Carlo searching technique, are efficient to determine the accurate critical slip surface of
54 the slope. Halder et al. [26] studied different analytical approaches and compared them with
55 finite element results to determine the accurate factor of safety for various slope angles and soil
56 types. Past research works have also been conducted to incorporate the uncertainty of soil
57 properties in the retaining wall design. Chogueur et al. [27] presents various simulations with
58 the structure installed into the supported ground without surcharge. They concluded that the
59 use of computational methods minimizes uncertainties arising from limited number of soil
60 properties. Muñoz-Medina et al. [28] searched for a suitable methodology for the selection of
61 retaining walls for different infrastructures and environments.

62 Up to date, only a few studies considered the uncertainties in soil properties with
63 respect to foundation. Sakleshpur et al. [29] searched for a method to incorporate uncertain soil
64 properties in the calculation of bearing capacity of shallow foundation. Somantri and Tarigan
65 [30] compared different methods to determine bearing capacity of pile foundation from the
66 results of dynamic analysis. Prayogo et al. [31] also investigated suitable methods to calculate

67 bearing capacity of pile based on the results of dynamic analysis. However, no study has been
68 conducted to accommodate the uncertainties with respect to bored pile capacity design.

69 The objective of this study is to develop a framework for the design of axial and lateral
70 capacity of bored pile in the area with limited soil parameters. The scope of study includes the
71 analytical calculation using different theories to accommodate the uncertainty due to the
72 limitation of site investigation data. The evaluation of the designed bored pile was carried out
73 using the commercial software for bored pile design.

74

75 **2. Site Overview and Methodology**

76 The proposed methodology consists of three main steps. In the first step, the properties
77 of the soil were estimated by correlation of SPT and CPT results, as will be discussed in details
78 in Section 3.

79 In the second step, the pile dimensions were estimated considering only its axial
80 resistance. The axial resistance of the pile was calculated using direct and indirect approaches.
81 In the former approach, the pile axial capacity was found through correlations of pile shaft and
82 tip resistance with the results of CPT and SPT, while in the latter one the axial capacity was
83 found by substituting the soil properties from the first step into the conventional methods, such
84 as alpha and lambda methods. A comparative analysis was conducted to select the method that
85 yielded the most conservative results from the two approaches. The analytical results were
86 further verified by numerical simulations using commercially available software, like GEO5
87 and RSPILE.

88 In the third step, the pile was designed for lateral capacity using three different methods:
89 p-y method, elastic analysis, and Brom's method. The pile-head deflections obtained by three
90 methods were compared to cross-validate the results of analysis. Figure 1 illustrates the
91 methodology.

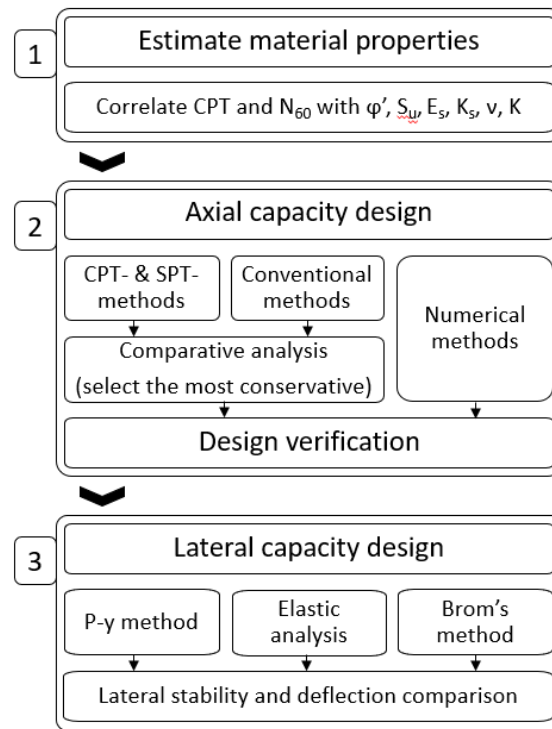


Figure 1. Flowchart of research methodology in this study

92
93
94
95
96
97
98
99
100
101
102
103
104
105
106
107
108
109
110
111

The proposed site is located at the intersection of Santa Monica Boulevard and S Moreno Drive, Los Angeles, USA. The project site is approximately 10,500 m² in plan. The site is flat without any slope. The geotechnical investigation of the site was performed by MACTEC Engineering [32]. The execution and design of project is challenged by the high seismicity, strong winds, and presence of deep clay layers at the site. Los Angeles is located at California Coast and is susceptible to severe earthquakes [33]. Over the past hundred years, several powerful earthquakes have struck the region, including the 1999 Hector Mine earthquake with a magnitude of 7.1, 1971 San Fernando earthquake with magnitude of 6.6, and 1952 Tehachapi earthquake with a magnitude of 7.5. According to data provided by ASCE [34], the speed of wind near the site is approximately 34 m/s for a 50-year mean recurrence interval. Since this value is higher than 30 m/s, the site location qualifies to be a “strong wind zone”. Wind direction in Los Angeles varies greatly throughout the year, but the most predominant directions from where wind blows are west (for 4.7 month), north (for 3.9 month), and south (for almost a month) (Weather Spark, n.d.). On average, the wind speed is the highest during the winter season, when wind blows mostly from the north; and it is the lowest during summer months, when wind blows mostly from the south direction.

The proposed construction site contains about 15 meters of soft clay layers. This can

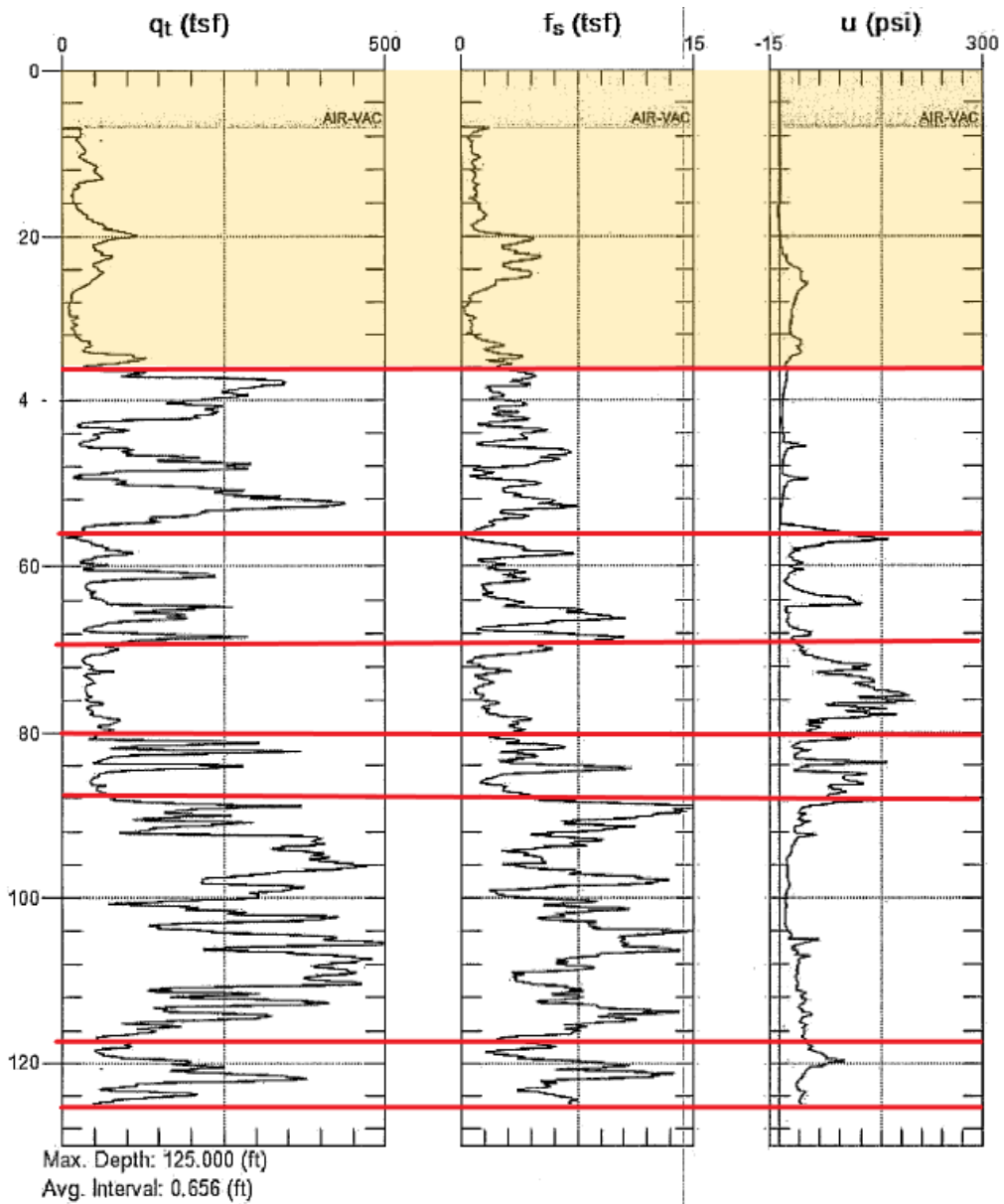
112 be interpreted from cone penetration test result as shown in Figure 2. This type of soil is
113 considered to be problematic in building construction [35]. Clayey soils tend to have low
114 bearing strength and therefore soil improvement or some special considerations in foundation
115 design will be required. In addition, clays are susceptible to shrinkage and volume expansion
116 depending on changes in moisture content, and they also consolidate over a prolonged period
117 of time due to sustained loads. These factors should be properly reflected in the geotechnical
118 design of the building to avoid significant changes in volume which may contribute to a
119 differential soil settlement, cracks in foundation, and permanent damage to the building.

120

121 **3. Determination of geotechnical parameters**

122 The geotechnical report, while providing valuable data on soil parameters, lacks
123 certain details. Therefore, it is necessary to correlate missing information from existing data.
124 The basis for majority of the correlations presented in this section were obtained using CPT
125 results. It is well established that CPT results can be used to obtain undrained shear strength,
126 internal friction angle, overconsolidation ratio, coefficient of lateral earth pressure, and many
127 more with a reasonable degree of accuracy [36].

128 The effective friction angle (ϕ') of cohesive soils was assumed to be zero under
129 undrained conditions and vertical loading [37]. The value of ϕ' for sandy soils was found using
130 four different methods from the values of q_c and N_{60} . The definitions of variables presented in
131 Table 1 are as follows: p_a is atmospheric pressure, σ'_0 is the effective stress. The estimated ϕ'
132 of sandy soils in the investigated site is summarized in Table 2. The estimated ϕ' were
133 compared with the typical values proposed by Look [38]. If the values of ϕ' were higher than
134 the range of ϕ' provided by Look [38], the values of ϕ' set to maximum ϕ' according to Look
135 [38] for conservative calculation.



136

137

138

Figure 2. Cone penetration test results from the investigated site

Table 1. Summary of correlation methods used for friction angle

Method №	Equation	Reference
1	$\phi' = \tan^{-1}(0.1 + 0.38 \log(\frac{q_c}{\sigma'_0}))$	[39]
2	$\phi' = 27.5 + 9.2 \log[N_{60}]$	[40]
3	$\phi' = \sqrt{20N_{60} + 20}$	[41]
4	$\phi' = \tan^{-1} \left(\frac{N_{60}}{\left(12.2 + 20.3 \left(\frac{\sigma'_0}{p_a} \right) \right)^{0.34}} \right)$	[42]

139

Table 2. Result of effective friction angle correlation (M in M1, M2, M3, M4 is abbreviation for Method)

Layer #	Depth interval (m)	Soil type	M ₁ ϕ'	M ₂ ϕ'	M ₃ ϕ'	M ₄ ϕ'	Average ϕ'	Typical range (Look, 2007)	Final ϕ' for analysis
2	2 – 4.1	Silty Sand	40	36	33	42	38	37-42	38
6	8 – 11	Silty Sand	32	37	35	36	35	37-42	35
7	11 – 17	Well-graded sand	39	41	45	48	43	40-43	43
12	29.1 – 33.8	Well-graded Sand	40	44	57	51	48	40-43	43
14	35.96 – 37.3	Silty Sand	35	43	50	44	43	37-42	42

140

141 The undrained shear strength of cohesive soils were determined using several methods
142 from CPT results as shown in Table 3. The definitions of variables presented in Table 3 are as
143 follows: s_u is the undrained shear strength, N_k and N_{kt} are the theoretical cone factors, σ_0 is
144 the total stress, q_t is the tip resistance from cone penetration test, f_s is the sleeve resistance
145 from cone penetration test. The typical values of N_k and N_{kt} for normally consolidated clays
146 have been reported to go up to 25 for overconsolidated clays [37]. In this study, upper range
147 values were taken for conservative design and analyses. Specifically, N_k was assumed equal to
148 20 for method 1 and 19 for method 2. The estimated undrained shear strength of cohesive soils
149 is presented in Table 4. As can be seen from the Table 4, the theoretical methods (methods 1
150 and 2) produce consistently higher values of the undrained shear strength as compared to the
151 multi-collinearity model (method 3), even with the application of conservative cone factors.
152 Therefore, the estimated undrained shear strength based on method 3 were utilized for
153 conservative design and analyses.

Table 3. Summary of correlation methods for undrained shear strength

Method №	Equation	Reference
1	$s_u = (q_c - \sigma'_0)/N_k$	[43]
2	$s_u = (q_t - \sigma_0)/N_{kt}$	[43]
3	$s_u = 0.070 * (q_t - \sigma_{v0})^{0.846} + 0.390 * f_s$	[44]

Table 4. Result of undrained shear strength correlation

Layer	Depth interval (m)	Soil type	Method 1 s_u (kPa)	Method 2 s_u (kPa)	Method 3 s_u (kPa)	Final s_u (kPa) for analysis
3	4.1-5.8	Sandy lean clay	163	172	102	102
4	5.8-7.6	Sandy silt	319	340	236	236
5	7.6-8.0	Sandy lean clay	181	201	172	172
8	17-21	Sandy silt	418	439	277	277
9	21-24.4	Clay	260	274	180	180
10	24.4-26.82	Sandy silt	615	646	347	347
11	26.82-29.1	Sandy silt	1061	1110	599	599
13	33.8-35.96	Clay	849	884	515	515
15	37.3-38.1	Sandy silt	471	484	358	358

154

155 The analyses of tip and shaft resistances of piles in sandy soils required earth pressure
 156 coefficient (K). The value of K was estimated using method proposed by Kulhawy and Mayne
 157 [39]. The estimated K for different sand layers in the investigated site is summarized in Table
 158 5. The estimated K are considerably higher than the typical K values specified in Tomlinson
 159 and Woodward [36]. The actual value of K may vary with depth. However, it was decided to
 160 use a limiting value of 1.0 for bored piles [36]. This would ensure safe design since high values
 161 of K would lead to excessive shaft and toe resistances.

Table 5. Effective earth pressure coefficients for sandy layers

Layer #	Depth interval (m)	Soil type	K	Final K to be used
2	2 – 4.1	Silty Sand	4.73	1.0
6	8 – 11	Silty Sand	1.75	1.0
7	11 – 17	Well-graded sand	5.73	1.0
12	29.1 – 33.8	Well-graded Sand	7.73	1.0
14	35.96 – 37.3	Silty Sand	3.56	1.0

162

163 The modulus of elasticity of soil (E_s) is a crucial parameter in the analyses of bearing
 164 capacity and settlement. This parameter was correlated from CPT and SPT results using Bowles
 165 (1996) model. The estimated E_s is summarized in Table 6. The values of estimated E_s were
 166 compared with the typical ranges provided by Bowles[45].

167 Poisson's ratio (ν) is a dimensionless ratio that measures the deformation in a material
 168 perpendicular to force direction. Typical ν is between 0.1 – 0.35 depending on the soil type [38].
 169 The values of ν were estimated using a qualitative method proposed by Kulwahy et al. [46].

Table 6. Result of elastic modulus correlation.

Layer	Depth interval (m)	Soil type	E _s typical, MPa [45]	E _s based on SPT, (MPa)	E _s based on CPT, (MPa)	Final E _s for analysis, (MPa)
1	0-2.0	Sandy lean clay	15-50	6	8	7
2	2.0-4.1	Silty Sand	7-21	48	48	48
3	4.1-5.8	Sandy lean clay	50-100	7	10	9
4	5.8-7.6	Sandy silt	7-21	7	7	7
5	7.6-8.0	Sandy lean clay	50-100	9	10	10
6	8.0-11.0	Silty sand	7-21	51	21	50
7	11.0-17	Sand	48-81	73	83	83
8	17-21	Sandy silt	7-21	9	9	50
9	21-24.4	Clay	50-100	10	45	50
10	24.4-26.82	Sandy silt	50-100	14	64	64
11	26.82-29.1	Sandy silt	50-100	22	108	108
12	29.1-33.8	Sand	96-192	110	178	196
13	33.8-35.96	Clay	50-100	20	87	87
14	35.96-37.3	Silty Sand	96-192	87	92	92
15	37.3-38.1	Sandy silt	50-100	16	10	50

170

171 The pressure sustained by soil per unit deflection was determined by the modulus of
 172 subgrade reaction (k_s). Vesic's method [47] was used to determine k_s . Table 7 summarizes the
 173 values of all the estimated soil properties.

174 Table 7. Summary of the estimated soil properties for geotechnical design of structure.

Interval	Depth interval (m)	Soil Classification	Undrained Shear strength s_u'	ϕ' ($^\circ$)	$\sigma'_{o, top}$ kPa	E _s , MPa	ν	k_s , kN/m ³
1	0-2.0	Cohesive (Sandy lean clay)	37.5	-	0	7	0.30	1906
2	2.0-4.1	Cohesionless (Silty Sand)	-	38	36	48	0.20	14542
3	4.1-5.8	Cohesive (Sandy lean clay)	102	-	72	9	0.30	2464
4	5.8-7.6	Cohesive (Sandy Silt)	236	-	102	7	0.30	1906
5	7.6-8.0	Cohesive (Sandy lean clay)	172	-	134	10	0.30	2804
6	8.0-11.0	Cohesionless (Silty Sand)	-	35	140	50	0.25	15565
7	11.0-17	Cohesionless (Sand)	-	43	184	83	0.30	27766
8	17-21	Cohesive (Sandy silt)	277	-	236	50	0.30	16035
9	21-24.4	Cohesive (Clay)	180	-	269	50	0.25	15565
10	24.4-26.82	Cohesive (Sandy silt)	347	-	290	64	0.30	20951
11	26.82-29.1	Cohesive (Sandy silt)	599	-	315	108	0.30	36931
12	29.1-33.8	Cohesionless (Sand)	-	43	337	196	0.35	73045
13	33.8-35.96	Cohesive (Stiff clay)	515	-	375	87	0.30	29219
14	35.96-37.3	Cohesionless (Silty Sand)	-	43	397	92	0.35	32192
15	37.3-38.1	Cohesive (Sandy silt)	358	-	410	50	0.30	16035

175

176 **4. Axial Capacity of Piles**

177 Load and resistance factor design (LRFD) method was used in the analysis since the
178 investigated site is located in the USA. A load combination stipulated in California Building
179 Code Section 1605.2 was used in the analysis [48]. The code provides a range of load
180 combinations and requires consideration of the most critical combination. For the case of axial
181 compression, the most critical combination from the code is 1.2(Dead Load) + 1.6(Live Load).
182 The dead and live loads from the upper structure were expected to be 489 kN and 116 kN,
183 respectively [49]. The total factored load on the foundation system is 520 MN. The LRFD
184 design requires that factored resistance of piles shall be less than or equal to the sum of shaft
185 resistance and toe resistance multiplied by their respective resistance factors [50].

186 The geotechnical resistance of piles should not exceed the structural capacity of the
187 piles themselves. In this study, bored concrete piles with the concrete compressive strength of
188 40 MPa, commonly used in industry, were assumed. The structural capacity of the pile (ϕP_n)
189 was calculated following ACI 318 (2014) ignoring contribution of reinforcing steel and
190 assuming tied pile ($\phi P_n = 0.35f_{cu}A_c$). A combined load factor of 1.4 provided a working load
191 of $0.25f_{cu}A_c$. The code of practice requires the design of foundation based on the highest load
192 from the column acting on a single pile (critical pile). In this study, the critical pile is located
193 at the center of the building. The required factored resistance for the critical pile is 9.63 MN.

194 Given the uncertainties on the soil conditions, a resistance factor of 0.333 [50] for the
195 toe and shaft resistance was adopted. This value corresponds to the lower bound of resistance
196 factors specified in AASHTO code (2007) and produces more conservative results. Two CPT-
197 based methods were used to calculate the toe and shaft resistances of piles. The first method
198 was originally published by Nottingham and Schmertmann [51] and later improved by
199 Schertmann [52] and included in FHWA-TS-78-209, "Guidelines for Cone Penetration Test,
200 Performance and Design". The second method was adopted based on study by Eslami and
201 Fellenius [53]. Upon completion of the analysis for a given pile diameter and embedment depth
202 using the two methods, the lowest values produced for both the shaft and toe resistance were
203 used to calculate the overall nominal bearing capacity of the pile.

204 In the first method, unit sleeve friction was correlated to nominal shaft resistance (R_s)
205 in cohesionless soil layers using Eq.1. The value of K_s was a function of q_c as well as ratio of
206 embedded pile depth to pile diameter and pile type. The R_s for cohesive soils was determined
207 using Eq. 2. Study by Nottingham [54] indicated that the calculation of the shaft resistance of

208 bored piles using Eq. 2 required the initially obtained nominal resistance taken as two thirds of
209 its original value. If driven piles are used, this adjustment is not necessary.

$$210 \quad R_s = K_s f_s A_s \quad (1)$$

211 where: K_s – ratio of unit pile shaft resistance to unit sleeve friction, f_s – average unit sleeve
212 friction over a depth interval, A_s – pile shaft surface area over f_s depth interval.

$$213 \quad R_s = \alpha' f_s A_s \quad (2)$$

214 where: α' – ratio of pile shaft resistance to cone sleeve friction, f_s – average unit sleeve friction
215 over a depth interval, A_s – pile shaft surface area over f_s depth interval.

216 The pile toe resistance was estimated based on the of averaging of cone resistance
217 values below and above the pile tip. Cone resistance values of 8 pile diameters above and 0.7
218 to 3.75 pile diameters below the pile tip should be used in the calculation [50]. In this study, an
219 average value of 2.25 $((0.7+3.75)/2)$ pile diameters below the pile tip was adopted.
220 Schmertmann [52] suggested an upper limit of 15 MPa on the tip resistance. During the
221 averaging procedure, geometric average of values was used as prescribed in AASHTO design
222 manual [55].

223 In the second method, the shaft resistance was also correlated to the average cone
224 resistance. However, effective cone resistance was used instead of q_c . The unit shaft resistance
225 was calculated using Eq. 3.

$$226 \quad f_s = C_s q_E \quad (3)$$

227 where: C_s – shaft correlation coefficient.

228 The calculation of the unit toe resistance based on the second method was determined
229 in a manner similar to that described in Schmertmann [52]. The difference is that the influence
230 zone at the pile tip ranges from 4b below the pile tip and 8b above where b is the pile
231 diameter/width. The unit toe resistance was calculated using Eq. 4. For pile diameters greater
232 than 16 inches (406 mm), the toe correction coefficient shall be determined from 12/b [50].

$$233 \quad q_p = C_p q_E \quad (4)$$

234 where: C_p – toe correction coefficient

235 The other methods were also used to calculate bearing capacity of the pile based on the
236 soil properties which were determined in Section 3. These methods, often called conventional
237 methods, are summarized in Table 8. Further details can be found in Das (2016).

238 According to alpha method, the shaft resistance (R_s) of bored pile is found from Eq. 5.
239 The summary of shaft resistances for each clay layer and total resistances within clay layer

240 surrounding pile based on alpha method is presented in Table 9. The value of C in Eq. 6 is
 241 suggested as 0.4 – 0.5 for bored piles [37]. In this study, 0.5 was used in the calculation of α
 242 following recommendation from American Petroleum Institute [63] for clay material.

$$243 \quad R_s = \alpha c_u p \Delta L \quad (5)$$

$$244 \quad \alpha = C \left(\frac{\sigma'}{c_u} \right)^{0.45} \quad (6)$$

245 where: c_u – undrained shear strength determined in Section 3, p – perimeter of pile, σ' –
 246 average effective vertical stress surrounding the pile, ΔL – thickness of clay layer.

Table 8. Summary of conventional method used to determine pile bearing capacity.

Rs	<ul style="list-style-type: none"> • Alpha (α) and gamma (γ) method for clays • calculation of bearing capacity for sands based on Das (2016)
Rp	<ul style="list-style-type: none"> • Coyle and Castello's method • Meyerhoff's method

247

248 Table 9. Shaft resistance based on alpha method for 25 m pile length and 0.5 m diameter.

Interval #	Z _{top} (m)	Z _{bot} (m)	ΔL (m)	$\sigma'_{o, top}$ kPa	c_u kPa	α	Rs, clay kN
3	17	21	4	235.78	276.68	0.465	808.86
4	21	24.4	3.4	268.99	180.04	0.599	575.98
5	24.4	26.82	2.42	290.20	347.27	0.461	608.81
6	26.82	29.1	2.28	315.11	311.00	0.503	560.21
Σ							2553.87

249 The determination of shaft resistance of bored pile based on gamma method was found
 250 using Eq.7. The summary of shaft resistance for each clay layer and total resistance within clay
 251 layer surrounding pile based on gamma method is presented in

252

253 The determination of shaft resistance of pile within sandy layers were performed using
 254 Eq. 8 (Das, 2016). The value of $K = 1$ was adopted in this study as explained in Section 3. The
 255 soil-pile interaction factor was taken as $0.8 \phi'$ following Das (2016). The summary of shaft
 256 resistance for each clay layer and total resistance within clay layer surrounding pile based on
 257 lamda method is presented in

258 Table 11.

259

260 Table 10. The gamma factor, γ , along pile embedment depth was taken as 0.150 (Das,
261 2016).

$$262 R_s = \gamma(\sigma' + 2c_u)p\Delta L \quad (7)$$

263
264 The determination of shaft resistance of pile within sandy layers were performed using
265 Eq. 8 (Das, 2016). The value of $K = 1$ was adopted in this study as explained in Section 3. The
266 soil-pile interaction factor was taken as $0.8 \phi'$ following Das (2016). The summary of shaft
267 resistance for each clay layer and total resistance within clay layer surrounding pile based on
268 lamda method is presented in

269 Table 11.

270
271 Table 10. Shaft resistance based on gamma method for 25 m long pile and 0.5 m in diameter.

Interval #	z_{top} (m)	z_{bot} (m)	ΔL (m)	$\sigma'_{o, top}$ (kPa)	c_u (kPa)	γ	R_s , clay (kN)
3	17	21	4	235.78	276.68	0.150	759.41
4	21	24.4	3.4	268.99	180.04	0.150	512.45
5	24.4	26.82	2.42	290.20	347.27	0.150	568.60
6	26.82	29.1	2.28	315.11	311.00	0.150	509.35
Σ							2349.82

$$272 R_s = K\sigma' \tan(\delta')p\Delta L \quad (8)$$

273 where: δ' – soil-pile interaction factor, K – effective earth pressure coefficient.

274
275 Table 11. Shaft resistance within sand layers for 25 m pile length and 0.5 m diameter.

Interval #	z_{top} (m)	z_{bot} (m)	ΔL (m)	ϕ'	δ'	K	f_s (kN/m ²)	R_s (kN)
1	8	11	3	35	28	1.0	74.58	351.44
2	11	17	6	42	34	1.0	122.54	1154.88
7	29.1	33.8	4.7	43	34	1.0	230.87	1704.43
Σ								3210.75

276 In this study, the toe of the pile was designed to be located within dense sand layer to
277 provide high resistance and to reduce settlement of the building. Therefore, the determination
278 of the toe resistance was conducted using Meyerhof [56] (Equation 9) and Coyle and Castello
279 [57] (Eq. 11). The limiting point resistance, q_L , is given by Eq. 10.

$$280 R_p = A_p q' N_q^* \leq A_p q_L \quad (9)$$

281 where: q' – effective vertical stress at the pile tip, N_q^* – bearing capacity factor which is a
282 function of friction angle (Das, 2006).

283
$$q_L = 0.5 p_a N_q^* \tan \phi' \quad (10)$$

284 where: p_a – atmospheric pressure (101.35 kPa)

285
$$R_p = A_p q' N^* \quad (11)$$

286 where: N^* – bearing capacity factor which is a function of friction angle and the embedment
 287 ratio (D/b) (Das, 2006), D – depth of pile, b – diameter of bored pile.

288 The value of N_q^* for Meyerhof's method was determined as 650 from the table in Das
 289 [37] for a soil friction angle of 43. Incorporating all required parameters for calculating toe
 290 resistance based on Meyerhof's equation, the toe resistance for bored pile with 25 m length and
 291 0.5 m diameter was 6020 kN. The value of N^* for Coyle and Castello's method was determined
 292 as 70. It should be noted that the determination of N^* provides the correlation for internal
 293 friction angles of up to 40°. Therefore, for all sandy layers where the friction angle was higher
 294 than 40°, a curve for 40° was used in the determination of the toe resistance with this method.
 295 Additionally, for this method, no limit on the toe resistance is stipulated in Das [37]. Therefore,
 296 limiting values proposed by Meyerhof [56] for piles in cohesionless soils were used.
 297 Incorporating all required parameters for calculating toe resistance based on Coyle and
 298 Castello's method, the toe resistance for bored pile with 25 m length and 0.5 m diameter was
 299 5145 kN.

300 As can be seen, among the conventional methods, Coyle and Castello's method
 301 produces more conservative results for the toe resistance. Therefore, the result from Coyle and
 302 Castello were utilized as toe resistance of pile and it was combined with the shaft resistance
 303 within clay layers from gamma method and the shaft resistance within sand layers from Das
 304 [37] method. The total resistance from this conventional method was compared with the total
 305 resistance from CPT results. The later method generated the lowest total resistance when
 306 Eslami and Fellenius [53] method was used. The comparison of total resistance from
 307 conventional method and CPT results is presented in Table 12. Compared to the conventional
 308 methods, the results of CPT-based method are more conservative in this case. With this
 309 observation, it was decided to proceed with the entire analysis using CPT-based methods.

310

311 Table 12. Comparisons of total resistance between different methods

Pile diameter	Conventional methods (MN)	CPT based method (MN)
1	11.77	6.54
0.75	7.32	5.09

0.5	3.57	3.54
-----	------	------

312

313

314

315

316

317

318

319

320

321

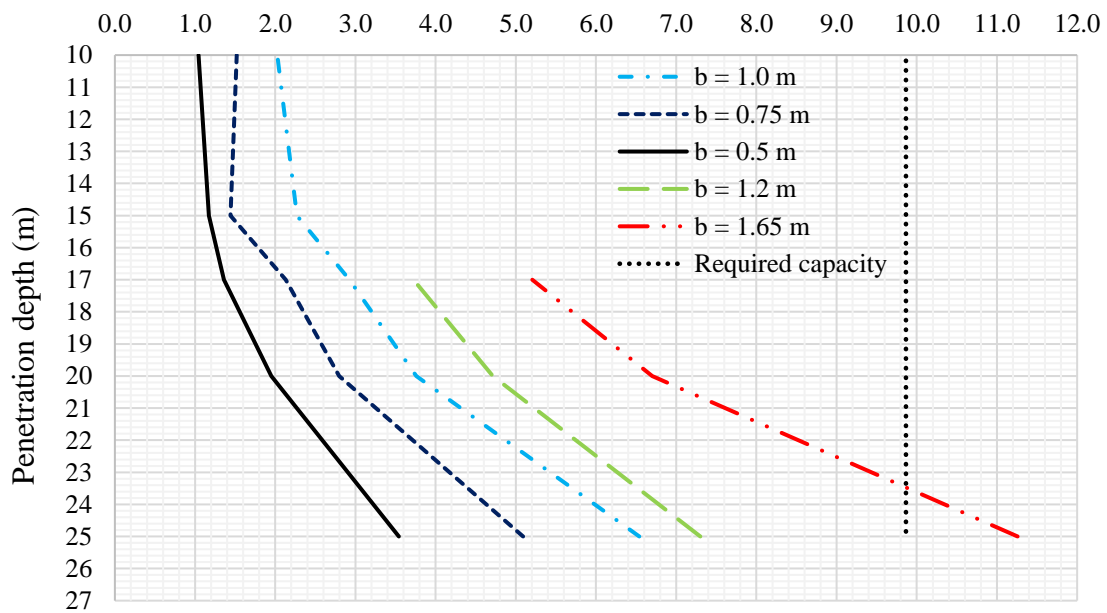
322

323

324

Overall, five pile diameters were considered in the analysis, i.e. 0.5, 0.75, 1.0, 1.2 and 1.65 m. It should be noted that these values are the standard sizes of boring tools which range from 600 mm to 2400 mm in 150 mm increment [58]. Figure 3 depicts the results of total resistance. From the figure a pile with a diameter of 1.65 m satisfies the bearing capacity requirement. This pile has a total factored bearing capacity of 11.26 MN (considering one pile per column). The required number of piles for the project was determined assuming a single pile per column. The total structural load was divided by the total resistance and was rounded up to estimate the required number of piles. Figure 4 shows the number of piles versus embedment depth for various design configurations. Upon doing a simple economic analysis based on cost data provided in Hannigan et al. [50], it was observed that group piles were uneconomical, and it was decided to proceed with single piled option of 1.65 m diameter pile (Figure 5).

Factored geotechnical resistance (MN)



325

326

Figure 3. Variations of total resistance for different penetration depths.

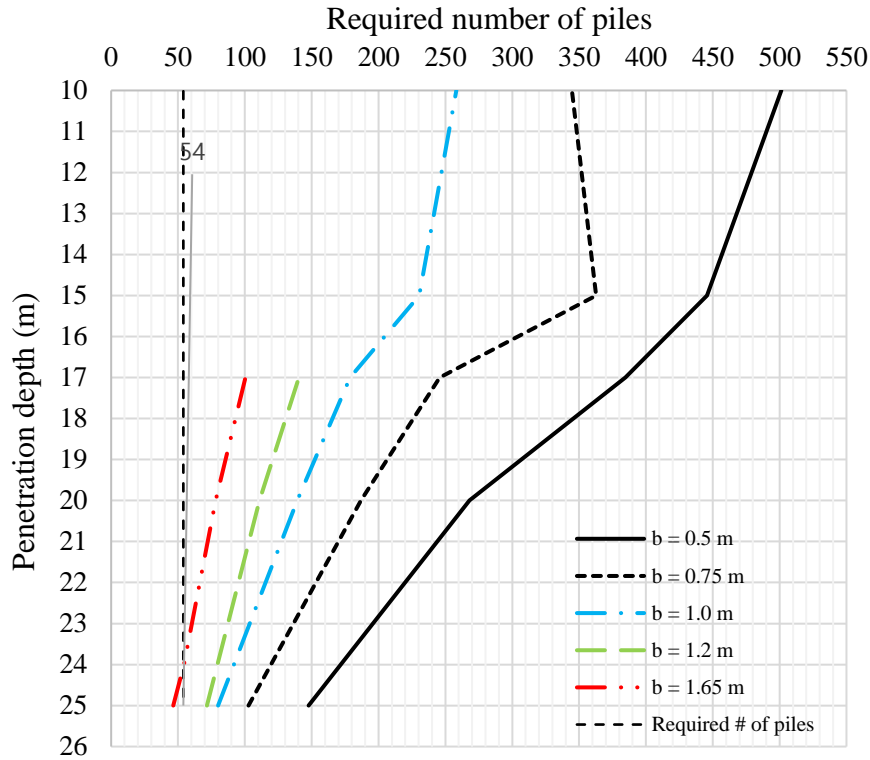


Figure 4. Required number of piles for different penetration depths.

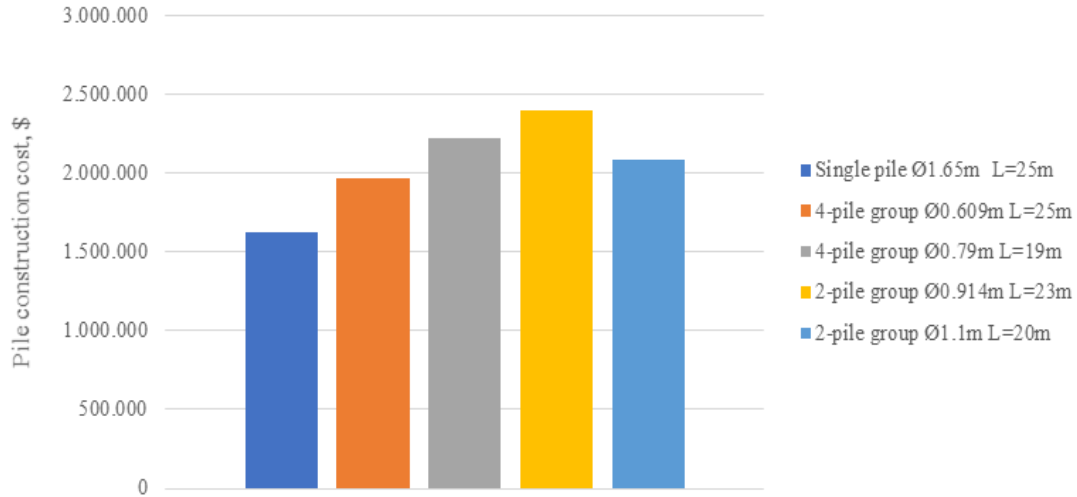
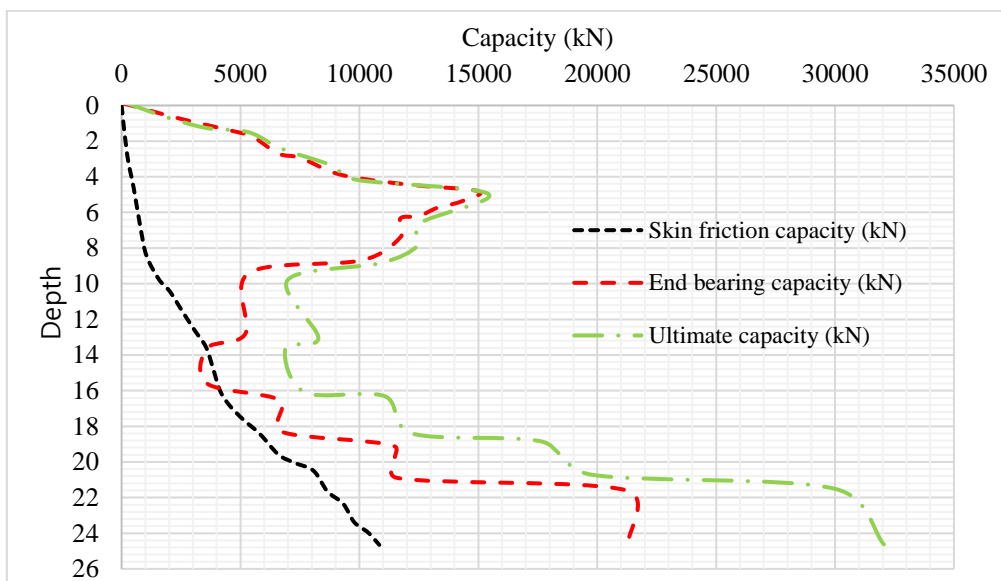


Figure 5. Comparison of cost for construction of foundation using pile group and single pile.

Commercially available GEO5 and RSPILE software [59-60] were used to verify the bearing capacity of the chosen pile. In RSPILE, the soil layers starting from the bottom of the basement were defined according to the soil properties in Table 7. The axial load was applied as factored axial compressive force on top of the pile. The results of the analysis in RSPILE is depicted in Figure 6. As can be seen from the results, upon dividing the ultimate pile capacity

338 by a safety factor of 3, the allowable capacity is equal to 10.74 MN, which is greater than the
339 factored load (9.865 MN).

340



341

342

Figure 6. Results of analyses from RSPILE.

343

344 In a similar manner, all necessary parameters including the pile dimensions, applied
345 loads and water table were defined in GEO5. However, in contrast to defining each soil layer
346 as in RSPILE, the digitized version of the CPT results was used. The software calculated the
347 bearing capacity based on the cone tip and sleeve friction values, the results of which can be
348 seen from Figure 7. Table 13 presents a summary of the results obtained by conventional
349 methods, CPT-based methods, and analysis using GEO5 and RSPILE. It is evident from the
350 results that the selected pile dimension ($D = 1.65$ m, $L = 25$ m) is sufficient to resist the factored
351 axial load effects.

352

353

Calculation of vertical pile bearing capacity - intermediate result

Pile diameter $d_{eq} = 1.65 \text{ m}$
 Pile diameter at base $d_{s,eq} = 1.65 \text{ m}$
 Pile area at base $A_b = 2.14 \text{ m}^2$
 Coeff. of reduc. of pile base bear. capacity $\alpha_p = 0.50$
 Coeff. of influence of pile shape $s = 1.00$
 Coeff. of influence of pile widened base $\beta = 1.00$

Calculation of vertical bearing capacity - results

Analysis carried out for test: Cropped starting from 0

Pile bearing capacity $F_{r,d} = 29917.18 \text{ kN}$
 Pile loading $F_{s,d} = 9685.18 \text{ kN}$

Safety factor = 3.09 > 3.00

Verification of pile for bearing capacity is SATISFACTORY

354

355

Figure 7. Results of analysis in GEO5

356

357

358

Table 13. Summary of axial bearing capacity of pile using multiple methods

	Conventional method	CPT-based method	Rspile	GEO5 Pile CPT
Design geotechnical capacity	16.16 MN	11.26 MN	10.74 MN	9.97 MN
	FS=5.0	FS = 3.488	FS = 3.327	FS = 3.089
	ok	ok	ok	ok

359

360

361

5. Lateral Capacity of Piles

363

364

365

366

367

368

369

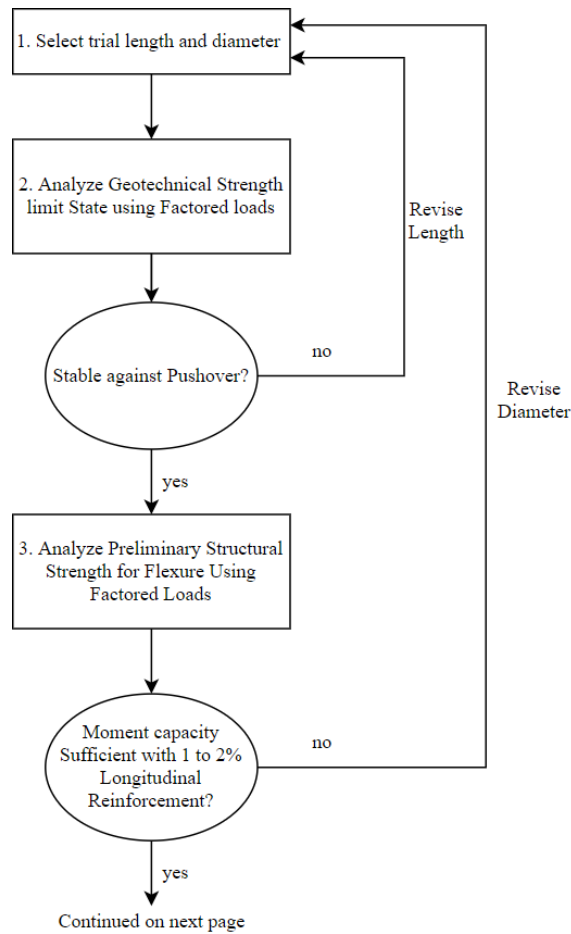
370

371

This part describes the analysis of the piles for lateral loading. The design procedure for the lateral analysis was adopted from the FHWA manual on drilled shafts [50]. The methodology can be seen from the design flowchart in Figure 8. The results of axial compression design of Section 4 were used for primary sizing of the piles and selection of embedment depth for lateral analysis. The majority of the analysis was performed using the LPILE [61]. With this software all the necessary components outlined in Figure 8 can be calculated. Additionally, non-linear analysis of the pile section using “p-y method” can be performed. This method is recommended for the purposes of lateral analysis of the piles [50]. The p-y method models the shaft as a nonlinear elastic beam and uses a series of nonlinear

372 springs to model the soil resistance. This model has been found to capture the essential
373 mechanisms of the problem and represent the soil-pile interaction [50].

374



375

376

Figure 8. Flowchart for Lateral analysis of Pile

377

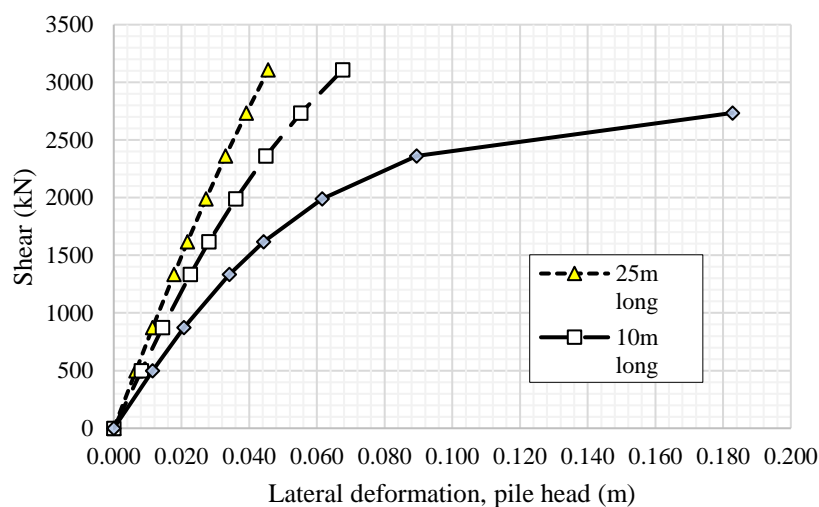
378 In order to analyze the geotechnical stability of the soil against lateral loads, pile
379 pushover analysis was performed. The analysis was done following the guidelines in FHWA
380 manual for drilled shaft foundation [50]. First, the pile shaft was modelled as a simple linear
381 elastic beam in LPILE with dimensions from the axial compression design. Uncracked cross
382 section of the pile was assumed. The properties of each soil layer were defined according to
383 the soil properties from Section 3. The built-in p-y curves of the program were used with API
384 sand (O’Neil) curve for cohesionless layers and Stiff Clay with Free Water (Reese) for cohesive
385 layers. These p-y curves are representative of the subsurface characteristics present at the site.

386 Once the model was established, to compute the deflections, lateral load was gradually
387 applied at the pile head in multiples up to and exceeding the factored load. A limit set for pile

388 deflection in FHWA manual was checked [50]. Although pile deflection is not the controlling
 389 parameter for checking the stability of the pile, the deflection from the analysis should not be
 390 greater than 10% of the shaft diameter as specified [50]. The last step in FHWA manual is to
 391 check the pile strength. To ensure sufficient strength reserve of the pile, a resistance factor less
 392 than one was recommended for lateral resistance. To incorporate this step into the software,
 393 loads up to $1/\phi$ the factored loads were applied on the pile head, where ϕ is the resistance factor
 394 of the soil. According to AASHTO 10.5.5.2.4-1 the recommended value for the factor is 1.0,
 395 the FHWA manual suggests a value of 0.67 for p-y method, which was used in this study [50].
 396 The results from the pushover analysis are presented in Figure 9.

397 From Figure 9, the results of the pushover analysis indicate that the chosen pile
 398 dimension ($D=1.65\text{m}$, $L=25\text{m}$) is sufficient to ensure stability of the soil. In fact, marginal
 399 stability was achieved with piles with an embedment depth of 8 meters. However, the 25-meter
 400 embedment depth was the required minimum to ensure necessary axial resistance as was
 401 explained in Section 4.

402



403

404

Figure 9. Results of pile pushover analysis

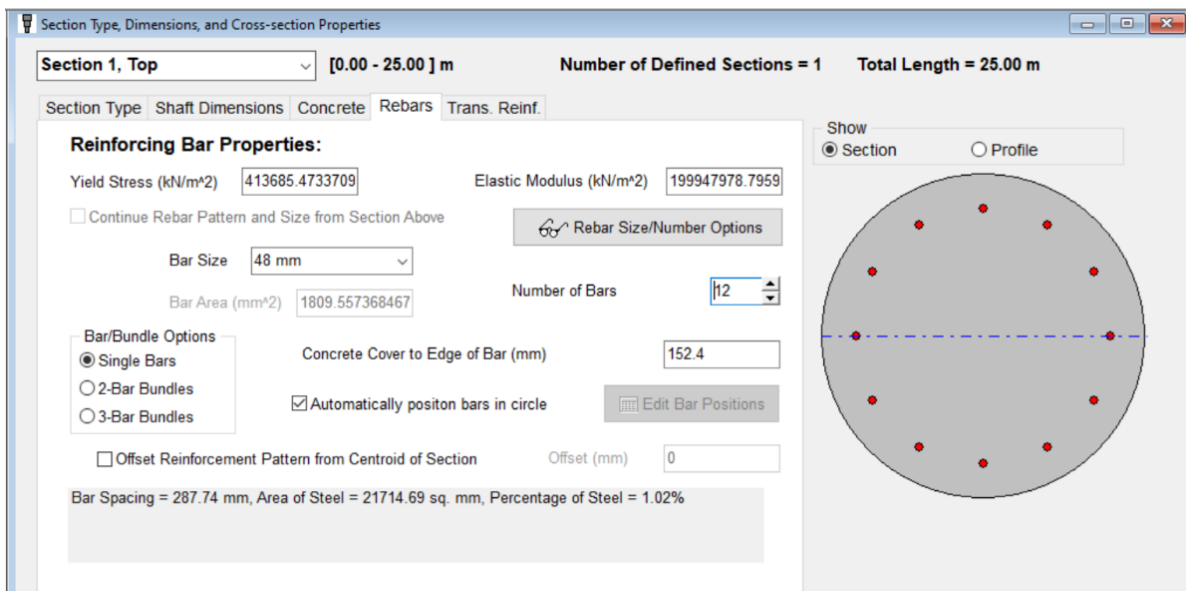
405

406 Structural Strength Limit State ensures that the designed shaft had sufficient size and
 407 length to withstand the imposed factored loads. In this stage of the analysis, the maximum
 408 bending moment and shear force on the pile were determined for the purposes of structural
 409 analysis. Additionally, preliminary check of flexural capacity of the pile were made. Similar to
 410 axial capacity design, LPILE was used to design of lateral capacity with nonelastic pile section
 411 and nominal 1.5% of reinforcement (Figure 10). The parameters for elastic modulus and yield

412 strength of the steel were left as default which were in line with the requirement in this study.
413 No transverse reinforcement was defined for this lateral analysis. The nominal moment
414 capacity of the section as determined by LPILE was 10786 kN-m or 9707 kN-m (including
415 factor) as shown in Figure 11. This value was higher than shear force (1842 kN) and bending
416 moment due to earthquake (7770 kN).

417 The LPILE can be used to determine the lateral deflection at the pile head. The
418 requirement for the lateral deflection limit was set to 25 mm [50]. Nonlinear pile section was
419 used in the analysis since in many cases a significant component of the deformation can be
420 related to flexural stiffness of the drilled shaft and not the ground response [50]. The result of
421 the analysis in LPILE indicate a pile head deflection of 0.01197 m or 11.97 mm as can be seen
422 from Figure 12.

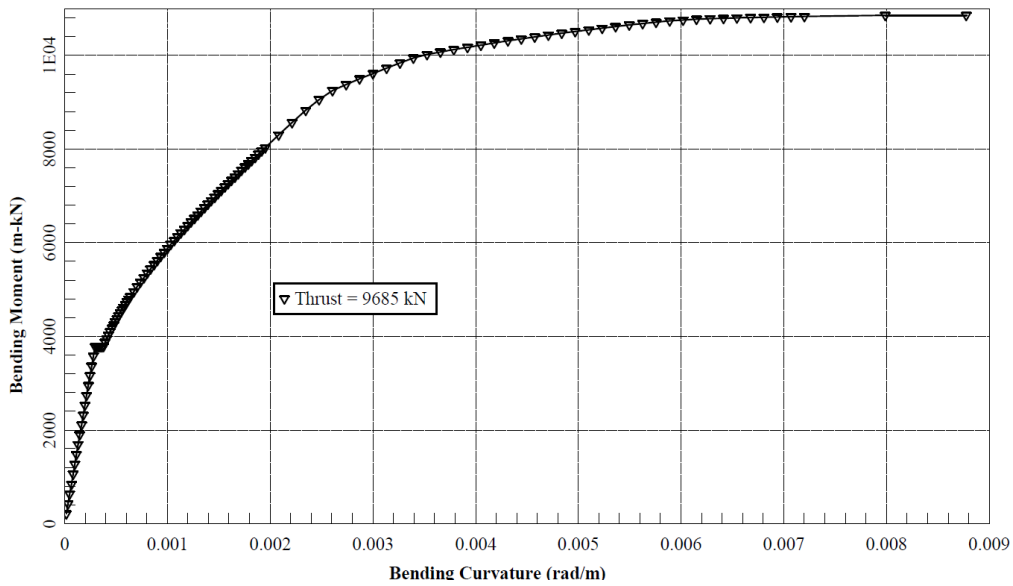
423



424

425

Figure 10. Nominal shear reinforcement properties for strength check

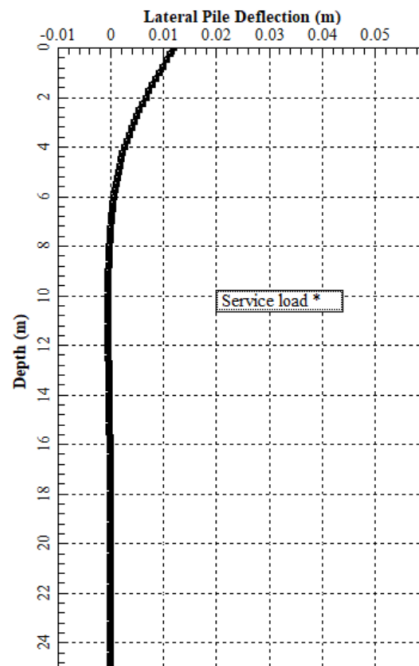


426

427

428

Figure 11. Bending moment vs. curvature



429

430

431

Figure 12. Lateral pile deflection vs. depth (LPILE)

432

433

434

435

436

437

In order to verify the results produced by LPILE, several other methods were used to check the pile head deflection at service loads. These include the analyses using GEO5 software, Excel spreadsheet, and hand calculation by Brom's method. In all of these alternative methods, a constant value of modulus of subgrade reaction (k_h) was used, which was determined using Vesic's method [62]. Additionally, pinned head conditions was assumed for all calculations to see the maximum theoretically possible head deflections.

438 The parameters for analysis using GEO5 were defined according to the soil properties
 439 stipulated in Section 3 and the pile dimensions were set as previously defined ($D=1.65\text{m}$,
 440 $L=25\text{m}$). The Excel spreadsheet provides a solution based on the assumption of elastic pile
 441 section with constant EI, constant soil stiffness in each element, and constant subdivision
 442 length. 25 elements (1 m per element) were defined in the spreadsheet and the values of k_h
 443 corresponding to each layer were input. The hand calculation involved the determination of
 444 ultimate pile loads and top deflections by Brom's method. It is a simplified method which
 445 assumes shear failure in soil for short piles, and bending of pile, governed by the plastic yield
 446 resistance of the pile section, for long piles. In the analysis, both cases were considered as
 447 recommended in the textbook by Das [62].

448 Table 14 summarizes the results obtained by all of the aforementioned methods. The
 449 maximum lateral deflection at the pile head ($=11.97\text{ mm}$) is well below the limit of 25 mm
 450 following requirement from FHWA [8]. Therefore, it can be stated the given pile dimensions
 451 are enough to satisfy the serviceability criteria. The comparative study indicated that the results
 452 from LPILE was higher as compared to results from other methods. It shows that the lateral
 453 analyses using LPILE provided more conservative value as compared to other methods.

454
 455 Table 14. Summary of pile head deflections for all analysis methods

	LPILE	GEO5	EXCEL	Das (2010)
y_{\max} (mm)	11.97	4.63	7.01	4.77

456

457 6. Conclusions

458 The main conclusions of this study are as follows:

- 459 1. The design of bored pile in the area with limited number of soil properties can be carried
 460 out as long as the consultant or contractor has the in-situ testing results from Standard
 461 Penetration Test (SPT) and Cone Penetration Test (CPT).
- 462 2. The determination of bearing capacity based on the axial load should include the
 463 calculation of skin friction and end bearing capacity using SPT and CPT results as well
 464 as the calculation of total axial capacity using alpha and lambda methods. The most
 465 conservative values from these methods should be used as the determination of the
 466 preliminary dimension of the pile based on the axial capacity
- 467 3. The design of final dimension of the pile should include the effect of the lateral capacity
 468 based on three methods: p-y curve, elastic analysis and Brom's method. The most

- 469 conservative values from these methods should be used as the determination of the final
470 dimension of the pile based on the lateral capacity
- 471 4. The appropriate partial factors based on relevant code of practice from USA (FHWA)
472 should be incorporated in the calculation of bearing capacity of the pile. In this study,
473 the results from cone penetration test and standard penetration test with code of practice
474 were used to design bored pile with 1.65 m diameter and 25 m depth.
- 475 5. GEO5, APile and LPile can based used to take into account the effect of axial load and
476 lateral loads in the calculation of bearing capacity.

477

478 **References**

- 479 [1] Zhou, H., Chen, Z. (2007). "Analysis of effect of different construction methods of piles
480 on the end effect on skin friction of piles." *Front. Archit. Civ. Eng. China* 1, 458–463.
- 481 [2] Das, I. and Stein, A. (2016), "Application of the Multitype Strauss Point Model for
482 Characterizing the Spatial Distribution of Landslides", *Mathematical Problems in*
483 *Engineering*, 1612901, 1-12.
- 484 [3] Joseph, A., Chandrakaran, S. and Jose, B.T. (2021), "Forensic Study of an Earth Retaining
485 System Failure." *Indian Geotechnical Journal* 51, 598–611.
- 486 [4] Rahardjo, H., Satyanaga, A., Leong, E.C., Ng, Y.S., Foo, M.D. and Wang, C.L. (2007)
487 "Slope Failures in Singapore due to Rainfall." *Proceedings of 10th Australia New Zealand*
488 *Conference on Geomechanics "Common Ground"*. Brisbane, Australia, 21-24 October,
489 Vol.2, pp. 704 - 709.
- 490 [5] Tokimatsu, K., Tamura, S., Suzuki, H., Katsumata, K., (2012). "Building damage
491 associated with geotechnical problems in the 2011 Tohoku Pacific Earthquake." *Soils*
492 *Found.* 52, 956–974.
- 493 [6] Karandikar, D.V. (2018), "Challenges to Quality Control in Bored Cast-In-Situ Piling in
494 Growing Urban Environment." *Indian Geotechnical Journal* 48, 360–376.
- 495 [7] Maniam Rajan, P., Krishnamurthy, P. (2019), "Termination Criteria of Bored Pile
496 Subjected to Axial Loading." *Indian Geotechnical Journal* 49, 566–579.
- 497 [8] Brown, D.A., Turner, J.P., Castelli, R.J., (2010). "Drilled Shaft: Construction Procedures
498 and LRFD Design Methods, FHWA NHI-10-016." *Federal Highway Administration, US*
499 *Department of Transportation, Washington, D. C.*
- 500 [9] Zhanabayeva, A., Sagidullina, N., Kim, J., Satyanaga, A., Lee, D., Moon, S.-W. (2021)
501 "A comparative analysis of Kazakhstani and European design specifications: raft

502 foundation, pile foundation, and piled raft foundation.” *Applied Sciences*, Mar,
503 11(7):3099.

504 [10] Gandhi, S.R. (2016), “Observations on Pile Design and Construction Practices in
505 India.” *Indian Geotech J* 46, 1–15.

506 [11] Gao, G., Zhuang, Y., Wang, K. and Chen, L. (2019) “Influence of Benoto bored pile
507 construction on nearby existing tunnel: A case study.” *Soils and Foundations*, 59(2):544-
508 555.

509 [12] Lam, C., Jefferis, S.A., and Suckling, T.P. (2014). “Construction techniques for bored
510 piling in sand using polymer fluids.” *Proceedings of the Institution of Civil Engineers -*
511 *Geotechnical Engineering*. 167:6, 565-573.

512 [13] Terwel, K.C. and Jansen, S.J.T. (2015). “Critical Factors for Structural Safety in the
513 Design and Construction Phase.” *Journal of Performance of Constructed Facilities*.
514 29(3):1-12.

515 [14] Satyanaga, A. and Rahardjo, H. (2020) “Stability of Unsaturated Soil Slopes Covered with
516 *Melastoma Malabathricum* in Singapore”. *Geotechnical Engineering*. 7(6):393-403.

517 [15] Satyanaga, A. and Rahardjo, H. (2020). “Role of Unsaturated Soil Properties in The
518 Development of Slope Susceptibility Map”, *Geotechnical Engineering*. 1-13.

519 [16] Zhang, J., (2009). “Characterizing Geotechnical Model Uncertainty.” *Hong University of*
520 *Science and Technology*.

521 [17] Ip., C.Y., Satyanaga, A. and Rahardjo, H. (2021). “Spatial variation of shear strength
522 properties incorporating auxiliary variables.” *Catena*, May, Vol 200, 105196

523 [18] Zhai, Q., H. Rahardjo and A. Satyanaga (2017) “Uncertainty in the estimation of
524 hysteresis of Soil-water Characteristic Curve”, *Environmental Geotechnics*, 6(4):204-213.

525 [19] Hettiarachchi H, Brown T (2009) “Use of SPT blow counts to estimate shear strength
526 properties of soils: energy balance approach.” *J Geotech Geoenviron Eng ASCE*, 135(6)

527 [20] Tan, M., Cheng, X. & Vanapalli, S. (2021) “Simple Approaches for the Design of Shallow
528 and Deep Foundations for Unsaturated Soils I: Theoretical and Experimental
529 Studies.” *Indian Geotechnical Journal* 51, 97–114.

530 [21] Singbal, P., Chatterjee, S. & Choudhury, D. (2020) “Assessment of Seismic Liquefaction
531 of Soil Site at Mundra Port, India, Using CPT and DMT Field Tests.” *Indian Geotechnical*
532 *Journal*, 50, 577–586.

533 [22] Orr, T.T.L. (2012). How Eurocode 7 has affected geotechnical design: a review
534 *Proceedings of the Institution of Civil Engineers - Geotechnical Engineering*. 165:6, 337-
535 350

- 536 [23] Vagnon F, Bonetto S, Ferrero AM, Harrison JP, Umili G. (2020). “Eurocode 7 and Rock
537 Engineering Design: The Case of Rockfall Protection Barriers.” *Geosciences*. 10(8):305.
- 538 [24] Becker, D.E., (1996). “Eighteenth Canadian geotechnical colloquium: Limit states design
539 for foundations. Part I. An overview of the foundation design process.” *Can. Geotech. J.*
540 33, 956–983.
- 541 [25] Alkasawneh, W., Husein Malkawi, A.I., Nusairat, J.H., Albataineh, N., (2008). “A
542 comparative study of various commercially available programs in slope stability analysis.”
543 *Comput. Geotech.* 35, 428–435.
- 544 [26] Halder, A., Nandi, S., Bandyopadhyay, K., (2020). “A Comparative Study on Slope
545 Stability Analysis by Different Approaches, in: *Lecture Notes in Civil Engineering.*”
546 Springer, Singapore.
- 547 [27] Chogueur, A., Abdeldjalil, Z., Reiffsteck, P., (2018). “Parametric and comparative study
548 of a flexible retaining wall.” *Period. Polytech. Civ. Eng.* 62, 295–307.
- 549 [28] Muñoz-Medina, B., Ordóñez, J., Romana, M.G., Lara-Galera, A., (2021). “Typology
550 selection of retainingwalls based on multicriteria decision-making methods.” *Appl. Sci.*
551 11, 1457.
- 552 [29] Sakleshpur, V.A., Satyanarayana Reddy, C.N.V., (2017). “A Comparative Study on
553 Bearing Capacity of Shallow Foundations in Sand from N and ϕ .” *J. Inst. Eng. Ser. A* 98,
554 355–365.
- 555 [30] Pile dynamic analyzer test and conventional analysis (Case on foundation bridge in
556 Cikampek), in: *IOP Conference Series: Earth and Environmental Science*.
- 557 [31] Prayogo, M.A., Wahyudi, H., Mochtar, I.B., (2021). “Comparison Between the Results of
558 the Pile Bearing Capacity Analysis Based on Empirical Method and Finite Element
559 Method Using the Results of Dynamic Analysis on the Field.” *J. Civ. Eng.* 36.
- 560 [32] MACTEC Engineering and Consulting, (2010). “Report of Geotechnical Consultation of
561 Proposed Melrose Triangle Mixed-use Project.” Los Angeles.
- 562 [33] USGS, (1985). “Evaluating Earthquake Hazards in Los Angeles Region - An Earth-
563 Science Perspective.” Washington.
- 564 [34] ASCE, (2020). ASCE 7 Hazard Tool [WWW Document]. URL
565 <https://asce7hazardtool.online/>
- 566 [35] Reddy, B.K., Sahu, R.B. & Ghosh, S. (2014) “Consolidation Behavior of Organic Soil in
567 Normal Kolkata Deposit.” *Indian Geotech J* 44, 341–350.
- 568 [36] Tomlinson, M., Woodward, J., (2014). “Pile Design and Construction Practice,” 5th ed.
569 Taylor & Francis Group, Boca Raton.

- 570 [37] Das, B.M., (2016). “Principles of Foundation Engineering,” 8th ed. Cengage Learning,
571 Boston.
- 572 [38] Look, B. (2007). “Handbook of Geotechnical Investigation and Design Tables,” Taylor &
573 Franics Group.
- 574 [39] Kulhawy, F.H., Mayne, P.W., (1990). Manual on Estimating Soil Properties for
575 Foundation Design. Ostigov.
- 576 [40] Kulhawy, F.H., Chen, J.R., (2007). Discussion of “Drilled Shaft Side Friction in Gravelly
577 Soils” by Kyle M. Rollins, Robert J. Clayton, Rodney C. Mikesell, and Bradford C. Blaise.
578 J. Geotech. Geoenvironmental Eng. 133.
- 579 [41] Hatanaka, M., Uchida, A., (1986). “Empirical correlation between cone resistance and
580 internal friction angle of sandy soils.” Soil Found. Louisiana State University.
- 581 [42] Schmertmann, J., (1975). “Measurement of In Situ Shear Strength.” Proc. Conf. in-situ
582 Meas. soil Prop. Am. Soc. Civ. Eng. II.
- 583 [43] Rocscience Inc., (2016). CPT Data Interpretation Theory Manual 1, 18.
- 584 [44] Hossain, M.I., (2018). Evaluation of Undrained Shear Strength and Soil Classification
585 from Cone Penetration Test.
- 586 [45] Bowles, J.E., (1996). Foundation Analysis and Design, 5th ed. McGraw-Hill, Singapore.
- 587 [46] Kulhawy, F.H., Trautmann, C.H., Beech, J.F., O’Rourke, T.D., McGuire, W., Wood, W.A.,
588 Capano, C., (1983). Transmission line structure foundations for uplift-compression
589 loading. Ithaca.
- 590 [47] Vesic, A.S., (1961). Bending of Beams Resting on Isotropic Solid. J. Eng. Mech. Div. Am.
591 Soc. Civ. Eng. 87, 35–53.
- 592 [48] California Building Standards Commission, (2008). California Building Code.
- 593 [49] Oralbek, A., Oteuil, A., Nazipov, F., Kobeyev, S., Mukhamet, T., (2021). “Design of a
594 High-rise Hotel in Los Angeles, California, USA.” Capstone Project Report, Nazarbayev
595 University, Nur-Sultan.
- 596 [50] Hannigan, P.J., Rausche, F., Likins, G.E., Robinson, B.R., Becker, M.L., (2016). FHWA-
597 NHI-16-009. Design and Construction of Driven Pile Foundations – Volume I.
598 Washington DC.
- 599 [51] Nottingham, L., Schmertmann, J., (1975). An Investigation of Pile Capacity Design
600 Procedures. Research Report No. D629. Gainesville.
- 601 [52] Schmertmann, J., (1978). Guidelines for Cone Penetration Test: Performance and Design.
602 Report FHWA-TS-78-209. Federal Highway Administration, Washington, D.C.
- 603 [53] Eslami, A., Fellenius, B.H., (1997). “Pile capacity by direct CPT and CPTu methods

604 applied to 102 case histories.” *Can. Geotech. J.* 34, 886–904.

605 [54] Nottingham, L.C., (1975). *Use of Quasi-Static Friction Cone Penetrometer Data to Predict*
606 *Load Capacity of Displacement Piles.* University of Florida.

607 [55] AASHTO, (2007). *LRFD Bridge Design Specifications*, 4th ed. American Association of
608 *State Highway and Transportation Officials*, Washington. D.C.

609 [56] Meyerhof, G.G., (1976). *Bearing Capacity and Settlement of Pile Foundations.* *ASCE J.*
610 *Geotech. Eng. Div.* 102.

611 [57] Coyle, H.M. and Castello, R.R. (1981). “New Design Correlations for Piles in
612 *Sand.”ASCE Journal of Geotechnical and Geoenvironmental Engineering.* 107(GT7),
613 965-986.

614 [58] Skanska, (2010). *Large Diameter Bored Piles.* [WWW Document].
615 [https://doi.org/10.1016/0148-9062\(86\)90249-4](https://doi.org/10.1016/0148-9062(86)90249-4)

616 [59] Fine spol. s r.o., (2020). *Geotechnical Software GEO5.*

617 [60] Rocscience Inc., (2020). *RSPile.*

618 [61] Khodair, Y., Abdel-Mohti, A. (2014) *Numerical Analysis of Pile–Soil Interaction under*
619 *Axial and Lateral Loads.* *Int J Concr Struct Mater* 8, 239–249.

620 [62] Das, B., (2010). *Principles of Foundation Engineering*, 7th ed. Cengage Learning.

621 [63] American Petroleum Institute (API). (1993). *Recommended practice for planning,*
622 *designing and constructing fixed offshore platforms*, 20th ed. American Petroleum
623 *Institute*, Dallas, Tex.